SLAC-PUB-6313
August 1993
(A/E)

SLC and SLD—Experimental Experience with a Linear Collider*

The SLD and SLC Collaborations
represented by
Martin Breidenbach
Stanford Linear Accelerator Center
Stanford, CA 94309

ABSTRACT

The SLAC Linear Collider (SLC) is the prototype e^+e^- linear collider. This talk will consist of an introduction to SLC, a description of the strategy for luminosity, a description of the systems for the transport and measurement of the polarized electrons,† and a description of the present performance of the SLC and planned upgrades. The detector, SLD, and the status of the polarization asymmetry measurement A_{LR} will be described.

1. SLC

A simplified schematic of SLC is shown in Figure 1. A cycle begins with two bunches of e^- and two bunches of e^+ being "cooled" by synchrotron radiation damping in their respective damping rings. After 1/120 s, one bunch of e^+ and both bunches of e^- are kicked from the rings and transported to the linac. The e^+ and the leading bunch of e^- are accelerated to about 46.6 GeV. At the head of the linac, the bunches are split by a dipole and transported through the SLC arcs toward the Collider Experimental Hall. The bunches are focused in an extensive optical system to transverse sizes of order 1 μm at the interaction point (IP). The beams continue past the IP and are kicked into ejection transport lines and led to beam dumps.

*Work supported by Department of Energy contract DE–AC03–76SF00515
†The Polarized Electron Source will be described by C. Prescott, elsewhere in these proceedings.
*

Presented at the 2nd International Workshop on Physics and Experiments with Linear Colliders Waikala, Hawaii, April 26–30, 1993.

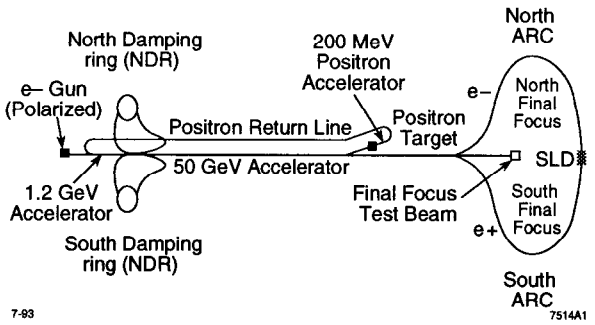

Figure 1. Simplified schematic of the SLC.

Meanwhile, the trailing e^- bunch was kicked out of the linac at approximately the 2/3 point and transported to an e^+ production target. The e^+ are collected, accelerated to 200 MeV, and transported back to the beginning of the linac. Here they are joined by two bunches of electrons from the Polarized Electron Source (PES) and accelerated to 1.2 GeV, where they are deflected into the appropriate transport lines and stored in their damping rings, thus beginning the cycle anew.

The luminosity L of a linear collider is

$$L = \frac{1}{4\pi} \frac{N^+ N^- f_c}{(\beta_x^* \beta_y^* \varepsilon_x \varepsilon_y)^{1/2}} H_D \eta$$

N^+ and N^- are the number of e^+ and e^- in each of the colliding bunches and f_c is the repetition frequency of the machine, 120 Hz for SLC. The denominator is essentially the spot size, here expressed as the square root of the products of the horizontal and vertical beta functions at the IP, multiplied by the emittance of the bunch. H_D is the disruption parameter describing a luminosity enhancement resulting from additional focusing of one beam in the electro magnetic field of the other. H_D is close to 1 for the present parameters of SLC, but should become important in the near future. Finally, η is an efficiency factor relating average luminosity over some macroscopic interval (days to weeks) to the peak luminosity described by this equation.

This simple equation is the guide for development of the strategies to improve the luminosity of the SLC. N^+ and N^- are nominally limited by the PES and the e^+ production system, with SLC requiring peak currents of amperes. Wake fields induced in the accelerator structure by the head of the bunch distort the tail of the bunch, degrading the beam emittance. Wake field effects are nonlinear in the bunch charge, increasing dramatically in SLC for currents above 5×10^{10}. Finally, the bunch charge may be limited by instabilities in the damping rings, which will be discussed later.

The collision frequency f_c is limited primarily by AC power distribution to the linac klystrons, and is essentially fixed for SLC. A strategy including raising f_c for SLC is not foreseen.

The $\beta_{x,y}^*$ are effectively the focal lengths of the final telescope before the IP. The values of β^* are limited by the bandwidth of the final focus system, since the energy spread within a bunch measures tenths of a percent. Various aberrations limit

the value of β^*, and attempts to adjust β^* to maximize luminosity can result in unacceptable backgrounds in the detector.

The emittances at the IP are limited by the damping ring performance, and by emittance growth caused by wake fields as the beams are accelerated down the linac and transported to the IP. Emittance growth from fluctuations of the synchrotron radiation in the arcs is relatively unimportant compared to wake field effects.

The disruption factor H_D is determined by the beam parameters, including the bunch length and the β^*. Disruption has not yet been observed at SLC, and no direct strategy to enhance H_D is planned.

The efficiency factor η, while not precisely defined, is extremely important. It includes not only operational availability of machine components, but also the stability required to tune and maintain machine parameters. Stability, in turn, depends both on understanding and achieving a vast set of component tolerances, and on complex feedback systems that maintain machine parameters—such as orbits and energies—with precision that can not be achieved through realizable component tolerances.

A convenient parameter to describe much of the machine is the specific luminosity Z_N formulated in units of Zs per hour as:

$$Z_N = \frac{L(Zs/hr)}{\left(\frac{N^+}{10^{10}}\right)\left(\frac{N^-}{10^{10}}\right)}$$

The goal of the 1993 SLC/SLD run is $(5-6) \times 10^4$ Zs recorded by SLD. At the beginning of the year, the strategy was to raise N^+ and N^- to around 4×10^{10}, and/or reduce ε_y by using flat rather than round beams from the damping rings.

Attempts to raise N^+ and N^- were found to be limited by unstable turbulent bunch lengthening in the damping rings.[1] This instability causes a slow sawtooth variation of the bunch lengths so that the bunch length at ejection into the linac is not predictable, and the collider becomes too unstable to operate. While the bunch lengthening could be controlled by a complex scheme of manipulation of the rf voltage of the damping ring, the effective maximum charge is $(3.1-3.2) \times 10^{10}$ per bunch. We believe that the instability is due to an impedance of the damping ring vacuum chambers that is too high. The cure is a new, smoother chamber with fewer shape transitions, and fabrication of such chambers is underway with installation planned for the fall of 1993.

The approach that has been more successful in 1993 has been to increase the specific luminosity by decreasing ε_y.[2] It is relatively simple to produce flat beams from the damping rings by shifting the operating point away from a coupling resonance. Figure 2 shows the beam size measured by wire scanners at the exit of the damping rings, achieving $\varepsilon_y = \varepsilon_x/10$. The vertical beam size is about 50 μm, compared with a horizontal size of about 200 μm.

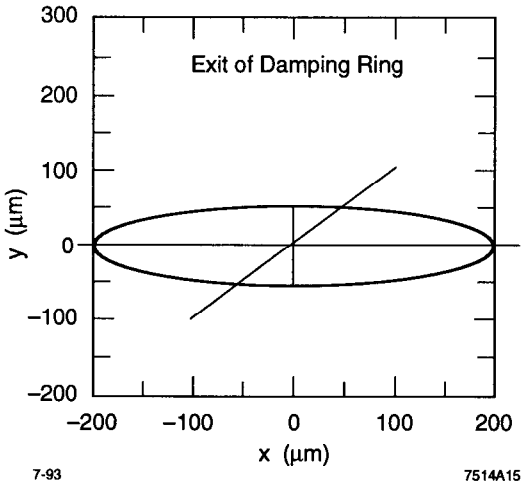

Figure 2. The beam size measured at the exit of the electron damping ring by a moving wire scanner. At this point, $\beta_x = \beta_y$ and $\epsilon_y = \epsilon_x/10$.

In contrast to production of the flat beam, preservation of the low emittance is challenging! The sensitivity of the bunches to wake field tails has required extensive detective work to uncover causes of random orbit deviations and the development of new techniques to deal with lower frequency disturbances. A few of these techniques will be briefly described.

Analysis of the time structure of linac orbit deviations,[3] by sampling significant fractions of the orbit at 120 Hz, revealed that there were accelerator quadrupole transverse vibrations with a dominant frequency of about 7 Hz, with peak-to-peak amplitudes of order 1 μm. These vibrations were traced to normal modes of the large aluminum girder that supports the actual accelerator structure, excited by broadband noise from cooling water loops. The vibrations were cured by addition of jacks and clamps to the support girder, eliminating the 7 Hz mode.

The SLC has developed an extensive set of feedback systems[4] that compensate for environmental effects ranging from diurnal temperature variations to beam orbit disturbances up to frequencies of tens of Hz. The feedback loops provide elegant ways of controlling final parameters, such as the beam energy, as well as maintaining optimal overlap of the two beams at the IP. Other features include stabilization against step changes, such as cycling and interchange of klystrons, or even isolation of operator tuning of one part of the machine from another. There are now about 50 feedback systems controlling about 150 parameters operating on the SLC.

Some of the SLC feedback systems are conceptually simple loops mediated by the host computer (for example, compensation of the main drive line length that fixes the phase of the linac klystrons), but many of the loops utilize multiple, rather powerful distributed computers to form Cascaded Adaptive Fast Feedback Loops. Such loops, for example, are used to stabilize the linac orbit, and involve large numbers of position monitors and fast steering dipoles. If one were to attempt to solve this problem with multiple independent loops, a disturbance would be multiply "corrected" by *all* loops downstream of the source of the disturbance, not just by the loop immediately downstream. *Cascading* of the loops means that measurements made by

upstream loops are propagated downstream, where they are combined with the local sensor data before corrections are calculated and the steering dipoles are set. An essential complication of this technique is the requirement of the downstream loop to "know" the effect of the upstream disturbance at the downstream sensor—that is, the transfer functions all along the machine must be known. While these transfer functions are initially determined by modeling, the modeling accuracy is not sufficient for these loops to perform well. Consequently, additional *adaptive* software continuously measures and corrects the transfer functions.

The orbit feedback loops can be used to introduce stable, deliberate bumps[5] in the linac orbit which cancel previously generated wake field tails. An example of such an orbit is shown in Figure 3.

The result of this work is illustrated in the time histories of Figure 4. Here the invariant emittances in X and Y of the e^- and e^+ are plotted for two-month periods centered on the transition to flat beams. The horizontal emittances at the end of the linac are approximately the same before and after the transition, but the vertical

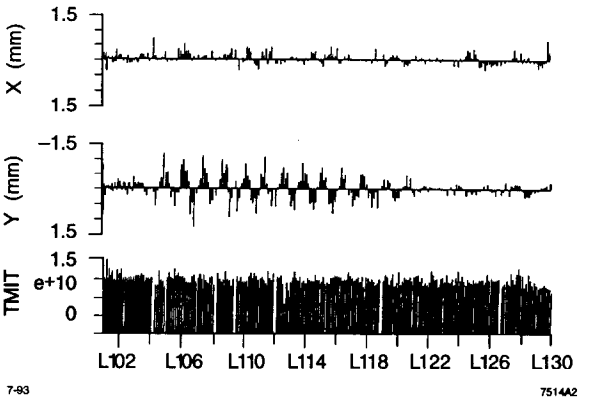

Figure 3. A beam position monitor scan of the linac for a single pulse of electrons. The oscillations are deliberate and used to cancel errors.

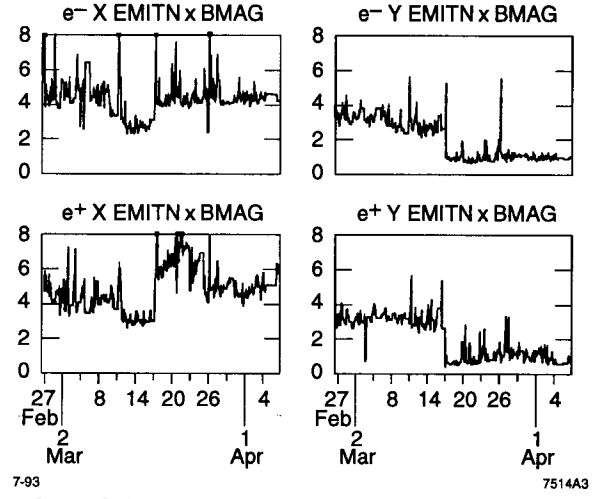

Figure 4. Time history plots of the vertical and horizontal emittances of the e^+ and e^- beams measured at the end of the linac. The transition to flat beams occurred in mid-March.

emittances drop from (3–4) to (0.7–0.8) $\times 10^{-5}$ radian meters. These emittances, with some effort, are now routinely maintained.

The beam size at the IP is measured by observing the deflection of the beams as they are scanned across each other.[6] The deflection angle Θ is proportional to

$$\frac{1 - e^{\frac{-\Delta x^2}{2\Sigma^2}}}{\Delta x},$$

where Δx is the separation of the beams and $\sum^2 = \sigma_+^2 + \sigma_-^2$ is the combined beam size along the direction of the deflection. Typical data of such a scan is shown in Figure 5. The above expression is fit to the deflection data to extract $\sum_x^2$ and $\sum_y^2$. Assuming the e^- and e^+ spots are of equal size, $\sigma_y \approx 800$ nm and $\sigma_x \approx 2.6$ μm are measured. (Carbon fibers measuring 7 μm can be inserted into the beam to measure an individual beam size, but the fibers are both too big and too fragile to be useful for these spot sizes and currents!)

The present (April 1993) luminosity performance of SLC is summarized in the time histories of Figure 6. These plots show measurements of N^+, N^-, Z_N and L over a period of a month. Z_N peaks of ≥ 5 are seen, compared to the 1992 best value of 2.8. Peaks of 6 to 7 are expected shortly. The actual luminosity peaks at about 40 Zs per hour. Figure 7 shows the complete SLC/SLD luminosity history. The 1991 detector engineering run recorded 300 unpolarized Zs. The 1992 run recorded 11,000 Zs with 22% beam polarization. The 1993 run (through April) has recorded 15,000 Zs with 55% average polarization. A feeling for the luminosity improvement is provided by the realization that a good day in 1993 records roughly twice as many Zs as in all of 1991.

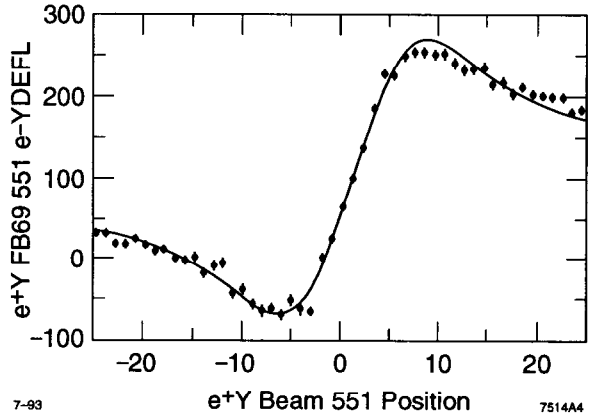

Figure 5. Plot of the deflection angle of the beams at the interaction point as a function of the e^+ beam position. The sum of the squared sizes of the bunches is calculated from a fit to these data.

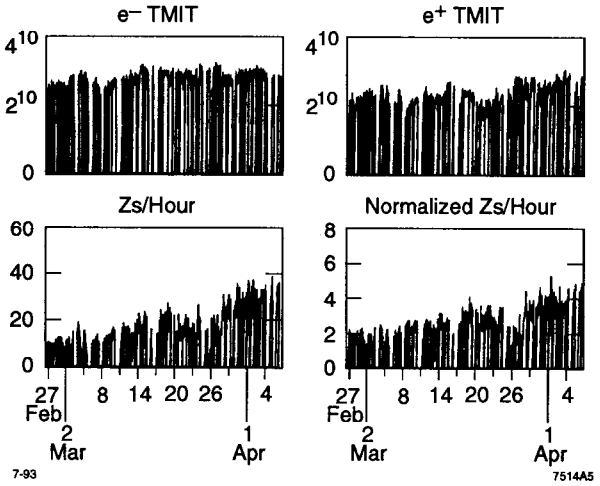

Figure 6. Time history plots of the e^- and e^+ bunch intensities, the normalized luminosity ZN, and the luminosity in units of Zs per hour. The transition to flat beams occurred in mid March.

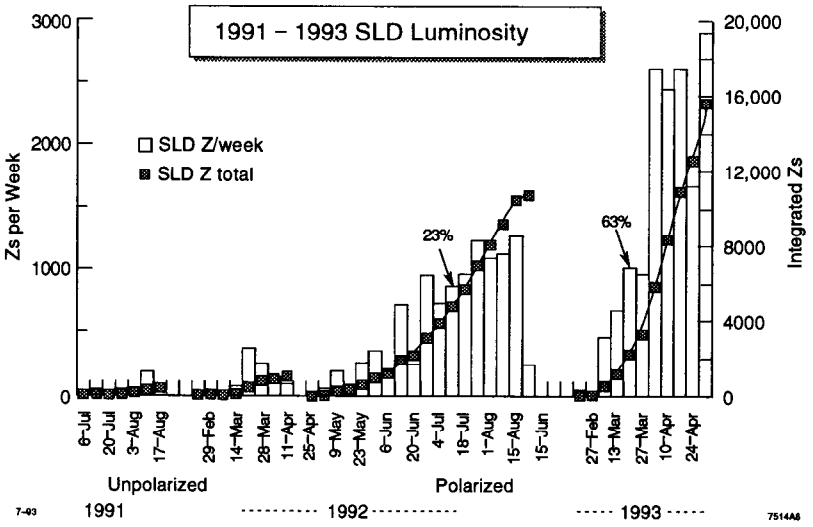

Figure 7. A complete history of the luminosity performance of SLC and SLD, indicating the luminosity in Z's per week and the integrated values for Z's actually recorded by SLD. The present performance in one day significantly exceeds that of all of 1991.

2. Polarization Transport and Measurement

A schematic of SLC showing the important features for operations with polarized e^- is shown in Figure 8. Longitudinally polarized e^- are generated by the source[7] and accelerated to 1.2 GeV. As the electrons are bent in the linac to ring (LTR) transport line, the spin precesses until it is transverse in the horizontal plane. A superconducting solenoid then rotates the spin to transverse vertical, so that it can be stored in the damping ring without depolarization. Before flat beams were introduced, an additional pair of spin rotation solenoids in the ring to linac (RTL) transfer line system and the linac were used to produce that spin orientation that would arrive longitudinal at the IP after going through about 70 spin rotations (about 25 net rotations) in the arc. The RTL spin rotators, however, would also rotate the spatial distributions of the electrons, and so cannot be used with flat beams. Fortunately, a method of introducing deliberate orbit bumps[8] in the electron arc to accumulate an arbitrary spin rotation in both dimensions was developed. Although sensitive to small orbit variations and requiring new feedback loops to achieve the necessary stability, this system is now routinely used to produce longitudinal polarization at the IP.

The polarization is measured by a Möller polarimeter at the end of the linac and by a Compton scattering polarimeter[9] just downstream of the IP. The Compton system is based on the difference in the $e\gamma$ cross section for parallel and anti-parallel orientations of the spin of the electron and the helicity of the photon from a circularly polarized laser beam. A 532-nm frequency doubled YAG laser is circularly polarized with a Pockels cell to produce left- or right-handed photons. The light is transmitted by a system of polarization compensated mirrors and lenses to the "Compton IP," about 32 m downstream of the SLD IP. The laser beam continues through the

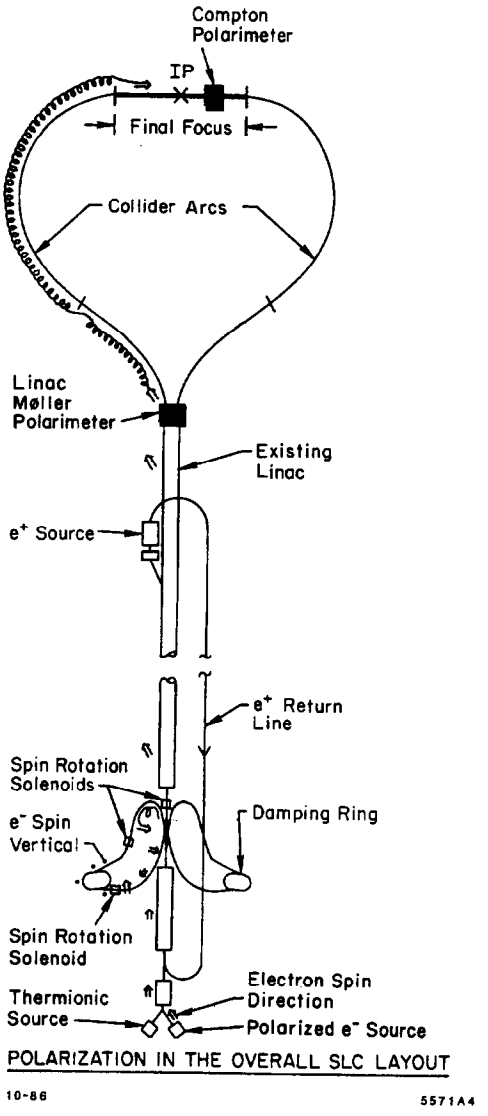

Figure 8. A simplified schematic of the SLC indicating those components that feature in the generation, transport, and measurement of polarized electrons.

beam line to a polarization analysis apparatus for measurement of the actual optical polarization. (This is an important issue, since uncertainty in the degree of optical polarization is the dominant contribution to the systematic error of the A_{LR} measurement.) The back-scattered Compton electrons are swept out of the exiting e^- beam in an analyzing bend magnet. The Compton electrons are then detected in redundant arrays of Cerenkov and proportional tube detectors. The Cerenkov detector has nine channels and the proportional tube detector has 16 channels, permitting the Compton edge and zero asymmetry point to be measured, and permitting a fit to the full Compton spectrum. The Compton system measures the polarization with a statistical

accuracy of 2% in a three-minute run, and is expected to have a systematic error of less than 2% by the end of this year.

The measured polarization at the Compton IP over a two-week period is indicated in Figure 9. Polarizations in the range of 60–64% are consistently achieved. The polarization from the PES is believed to be about 75%. Further improvements to the source are possible and are described by C. Prescott.[10] There is a small mismatch between the operating energy of the damping ring and design that results in about a 1% polarization loss from incomplete spin rotation to the vertical. The polarization loss in the arcs is 15–20% and is not understood. Possibilities for spin bumps that will minimize the depolarization are being studied.

3. Upgrade Program

Two significant machine upgrades have been approved for installation after completion of this run: new damping ring vacuum chambers and optics upgrades for the final focus.

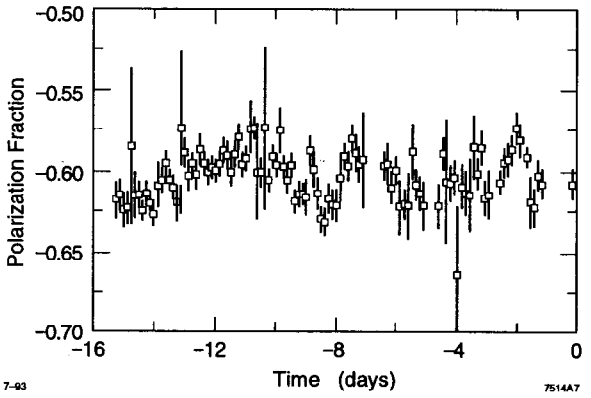

Figure 9. A time history of the polarization measured by the Compton Polarimeter at the IP during a representative two week period.

The new vacuum chambers will raise the intensity threshold for bunch lengthening so that $N > 4 \times 10^{10}$ at the IP may be achieved. In addition, the bunch length will be reduced, leading to further emittance reduction, and the energy spread should be reduced from $\sim 0.3\%$ to $\leq 0.2\%$, reducing the contribution of chromatic terms to the spot size (significant for the vertical spot size) and reducing the depolarization during transport through the arc.

The limitations of the current final focus[11] are indicated in Figure 10 where the vertical and horizontal spot sizes are plotted as a function of the beam divergence angle. Both the linear and the actual behavior (calculated up to third order aberrations) are shown. The difference in vertical spot size between linear and linear plus aberrations is particularly striking. At the current operating point of the final focus, the

linear contribution to the horizontal spot size is 71%, with a 23% contribution from a chromatic term. Conversely, the dominant contribution to vertical spot size is 86% from a particular chromatic aberration, and only 3% from the linear contribution. New quadrupoles and octupoles are planned to significantly reduce this aberration, and new diagnostics will be added to improve tuning. These improvements should reduce the vertical spot size below 500 nm and bring peak $Z_N > 10$. The history and expected progression of spot size reduction is indicated in Figure 11. It is interesting that the spot size passed design expectations this year.

With these spot sizes and currents, the pinch effect is calculated[12] to become significant. Depending on the precise choice of parameters, H_D should be in the range 1.4–1.6.

To summarize the expected peak luminosity improvements, the damping ring and final focus upgrades should give 190 Zs/hr, without including the beam disruption enhancement. This should permit more than 2×10^5 Zs to be recorded in a half-year physics run.

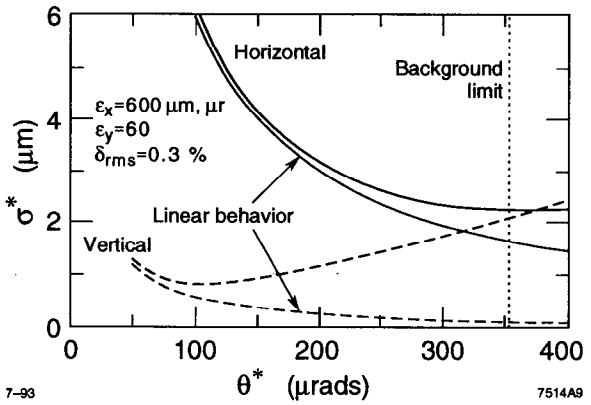

Figure 10. Plot showing the expected vertical and horizontal spot sizes (s) at the IP as a function of the beam divergence angles. Both the linear contribution and the sum through third order corrections are shown.

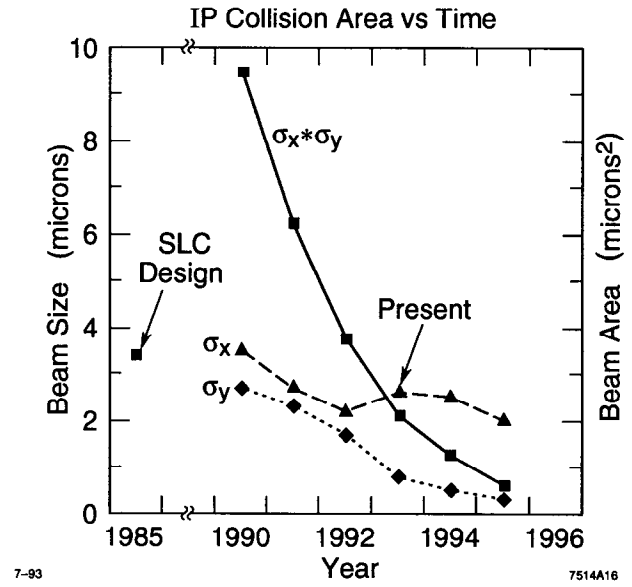

Figure 11. The history and expected progression of the SLC IP spot sizes and areas.

4. SLD

A schematic of SLD is shown in Figure 12. It is similar in scope and scale to the LEP detectors, but it is optimized for SLC. In particular, it has a 25-mm radius beam pipe surrounded by a CCD vertex detector, and Cerenkov Ring Imaging Detectors for particle identification. Its electronics are relatively simple, taking maximal advantage of the long time between beam pulses.

The high polarization of SLC significantly offsets the low luminosity of SLC relative to LEP in several areas of physics. The best-known measurement is the electroweak polarization asymmetry A_{LR}. The polarized forward-backward asymmetry provides a powerful $b - \bar{b}$ tag, which should make extremely competitive b-mixing

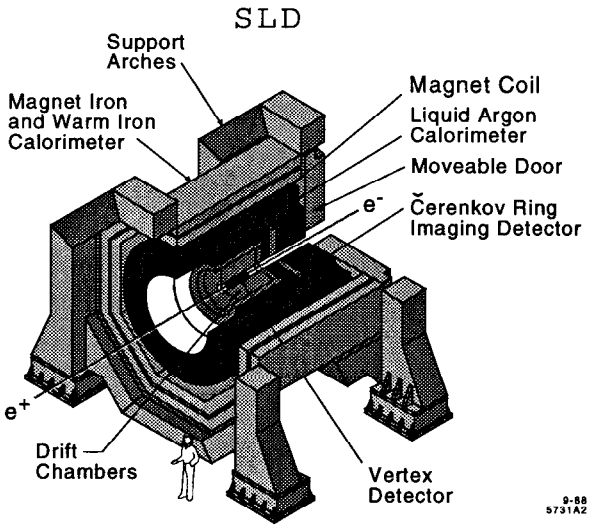

Figure 12. Cutaway view of SLD.

measurements possible. The pixel-based high-resolution vertex detector is significant in many areas of b physics. Many QCD topics are limited by theoretical uncertainties, and the smaller SLC/SLD Z sample does not hurt. Other QCD topics take advantage of the polarization.

The first measurement of the left-right cross section asymmetry A_{LR} in the production of Z bosons in e^+e^- collisions was performed by SLD using the polarized electron beam from SLC in 1992.[13] The measured asymmetry is

$$A_{LR}^{meas} = PA_{LR} = P\left(\frac{\sigma_L - \sigma_R}{\sigma_L + \sigma_R}\right)$$

where σ_L and σ_R are the e^+e^- production cross sections for Zs with left- and right-handed electrons, and P is the longitudinal polarization of the electrons. In the Standard Model, A_{LR} depends on the vector and axial vector couplings of the Z to the electron current:

$$A_{LR} = \frac{2a_e v_e}{a_e^2 + v_e^2} = \frac{2[1 - 4\sin^2\theta_w^{eff}]}{1 + [1 - 4\sin^2\theta_w^{eff}]^2}$$

In contrast, the unpolarized forward-backward asymmetries accessible to the LEP experiments measure the product of the Z couplings to the electron and to the final state fermion:

$$A_{FB} = \frac{\sigma_F - \sigma_B}{\sigma_F + \sigma_B} = \frac{3}{4}A_f A_e.$$

The forward-backward asymmetries have rather different sensitivities to $\sin^2\theta_W^{eff}$ compared to the left-right asymmetry. For $W = \sin^2\theta_W^{eff} \approx 0.23$, the leptonic forward-backward asymmetries $A_{FB}^l = \frac{3}{4}A_l A_e$ have $\delta A_{FB}^l \approx -1.9\delta W$. The b quark asymmetry, with different b couplings, has $\delta A_{FB}^b \approx 5.6\delta W$. The left-right asymmetry has $\delta A_{LR} \approx 7.8\delta W$. This helps make measurements of the weak mixing angle very competitive despite the luminosity advantage at LEP.

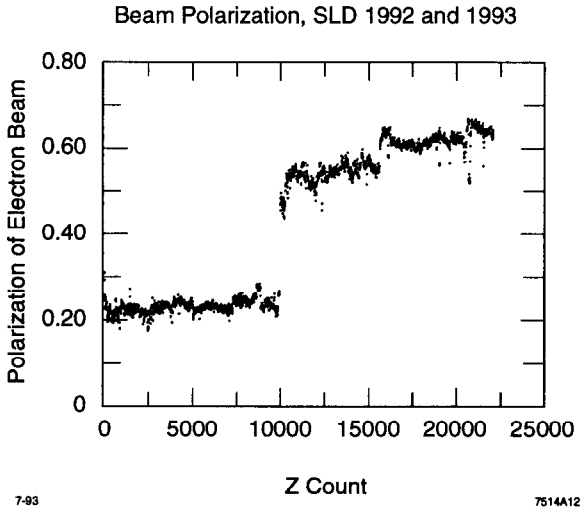

Figure 13. A plot of the electron polarization associated with each Z used in the A_{LR} measurement. The first set of data with a polarization around 22% corresponds to a bulk GaAs photocathode in the electron gun. The second set corresponds to the introduction of a strained lattice GaAs photocathode, and the step corresponds to an increase in the wavelength of the photocathode illumination.

The precision of the A_{LR} measurement is given by $\delta A_{LR}^2 = \left(\frac{\delta P}{P}\right)^2 A_{LR}^2 + \frac{1}{P^2 N}$, and for a polarization of 60% measured with 1% systematic error, the error is dominated by statistics until roughly 10^6 Zs are recorded. All final states except Bhabhas are used in the measurement. The measurement is robust in the sense that the hadronic Z events are simply counted for each polarization state—A_{LR} is insensitive to effects of absolute luminosity, detector acceptance, and detector efficiency. Of course, the A_{LR} measurement does require the absolute measurement of the polarization by the Compton polarimeter.

The beam polarization for all of our data is shown in Figure 13. Here a polarization value is plotted for each accepted Z. The first 10^4 events at 22% polarization are from the 1992 data using a bulk GaAs photocathode in the source. In 1993, the photocathode was replaced with one made from strained GaAs, resulting in a polarization at the detector of approximately 55%. After the next 5,000 Zs, the laser wavelength illuminating the photo cathode was increased to approximately 860 nm, increasing the polarization to about 62%.

Figure 14 shows the directly measured asymmetry from the 1993 data for Zs and for small-angle Bhabhas. The Z asymmetry is large, around 10% for the 60% polarized beams. The Bhabha asymmetry, extracted from the same blocks of data as for the Zs, is used as a check. The Bhabha asymmetry is consistent with 0, and is expected to be of the order 10^{-4}.

The 1993 data are still being analyzed, and an A_{LR} value is not yet available. The 1992 data were recently published, with $A_{LR} = 0.100 \pm 0.044$ (stat) ± 0.004 (syst). This result is based on 5,226 Zs from left-handed electrons and 4,998 Zs from right-handed electrons, with a luminosity weighted polarization of $(22.4 \pm 0.6)\%$. This value of A_{LR} corresponds to $\sin^2 \theta_W^{eff} = 0.2378 \pm 0.0056(stat) \pm 0.0005(syst)$.

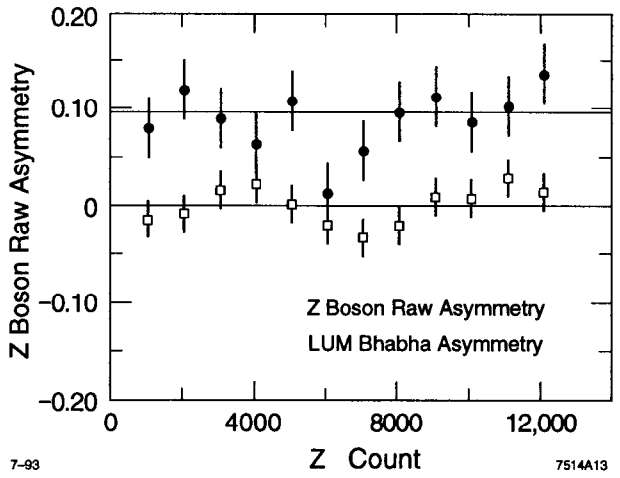

Figure 14. The directly measured asymmetry (uncorrected for the actual polarization value) for Zs and Bhabhas from the 1993 data.

Figure 15 shows the expected error in the weak mixing angle determined by the A_{LR} measurement as a function of the number of Zs logged. Approximate time markers corresponding to the 1993 and 1994 data runs are shown. An ultimate error around 0.0003 is expected, comparable to limits from theoretical errors on the radiative corrections.

Time does not permit a discussion here of other physics analyses by SLD using SLC. However, brief mention of the Vertex Detector[14] is appropriate since it takes full advantage of the small beam pipe possible with SLC. Figure 16 is a photograph, taken before final assembly, of the two halves of the Vertex Detector. The detector is built up in two layers from 64 ladders, each containing 8 CCDs with active areas of 10 mm × 12 mm. The CCDs are arrays of pixels 20 μm on a side, yielding fully two-dimensional position measurements of charged particles with a resolution of about 5 μm. The beryllium beam pipe radius is 25 mm. The performance of the system is characterized by an impact parameter resolution of $(13 \oplus \frac{70}{P sin^{3/2}\theta})\mu m$ in the transverse plane and $(52 \oplus \frac{70}{P \sin^{3/2}\theta})\mu m$ in the plane containing the beam line. The mean beam position can be measured with an error of about 11 μm. The range of physics accessible to SLC/SLD in the next several years is summarized in Table 1. Each topic is shown with the current world average and the expected precision from an SLC/SLD run of 10^6 Zs with an electron polarization of 65%.

5. Conclusions

• SLC works at luminosities required for competitive physics. Electron polarization $\geq$ 60% at the detector is routine. The combination of high polarization and reasonable luminosity makes compelling physics accessible in the major areas of precision electroweak measurements, studies of heavy flavor, and QCD measurements.•

• Linear colliders are very difficult machines. In contrast to storage rings, they are inherently unstable, and extremely dependent on feedback systems and other controls to achieve stable operation. Machine optimization is made difficult by important non-linear effects, such as wake fields and damping ring instabilities. In the final focus,

third-order optical effects dominate the vertical spot size. Mechanical tolerances tend to be very tight. Nevertheless, many significant problems appear to be resolved. The linac klystrons, operating at 50 MW peak power at S Band, were a significant concern during the design of the machine, but have proved to be a very reliable power source. The polarized electron source, which presented problems for many years, seems to be under control, with perhaps 10% more polarization expected in the near future. Positron production, again once a significant problem, is now routine, with net yields of one positron out of the damping ring per electron on the positron target.

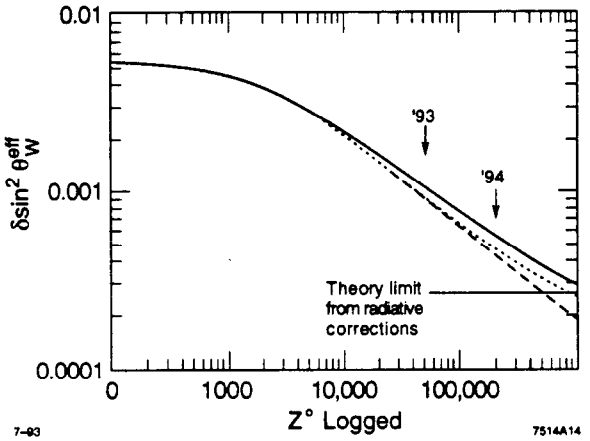

Figure 15. The expected error in the weak mixing angle as a function of the number of recorded Zs. The expected error in the weak mixing angle as a function of the number of recorded Z's. The solid line corresponds to a mean polarization of 54% and a 1% polarization measurement error. The dashed line is the same polarization with no measurement error. The dotted line is for polarization going from 54% to 62% during the first 50 K events, going to 68% thereafter, all with 1% measurement error.

Figure 16. A photograph of the two halves of the Vertex Detector before final assembly.

Table I

A summary of the proposed SLD Physics Program. Each measurement is listed along with the parameters that are extracted from the measurement, the current value of the parameter, and the precision that is obtainable by SLD with a sample of 10^6 visible Z's with $\mathcal{P}_e = 65\%$.*

Measurement	Parameter	World Average*	SLD (10^6 Z)
A_{LR}	$\sin^2\theta_W^{\rm eff}$	0.2318±0.0007	0.00027
$\tilde{A}_{FB}^{\mu}$	v_μ/v_e	$0.85^{+0.27}_{-0.22}$	0.08
$\tilde{A}_{FB}^{\tau}$	v_τ/v_e	$1.04^{+0.17}_{-0.14}$	0.08
τ lifetime	τ_τ	297±3 fs	$\lesssim$3 fs
τ charged current	h_ν	$1.25\pm0.23^{+0.15}_{-0.08}$	0.03
"	ξ	0.90±0.15	0.10
"	δ	—	0.10
b partial width	R_b	0.22±0.003	0.002
c partial width	R_c	0.17±0.017	0.004?
$\tilde{A}_{FB}^{b}$	A_b	0.90±0.09	0.02
B lifetime	τ_B	149±6 ps	~5 ps
B^+/B^0 lifetime	R_τ	$0.96^{+0.19+0.18}_{-0.15-0.12}$	~0.05
B_s Mixing	$f_{B_s^0}$	—	$f_{B_s^0}/4.2$
"	x_s	—	$0.1\cdot x_s$
flavor ind. of α_s	$\alpha_s(b)/\alpha_s(udscb)$	1.01±0.04	~0.01
"	$\alpha_s(c)/\alpha_s(udscb)$	—	~0.01
Q_h assoc. mult.	$\bar{n}_b$	23.1±1.9	~0.2
"	$\bar{n}_c$	—	~0.2
$g\to q\bar{q}$ vertex	$r{=}\Gamma_{4Q_h}/\Gamma_{2Q_h}$	—	$\sim 0.05\cdot r$
g/q color charges	$\langle n\rangle_g/\langle n\rangle_q$	1.27±0.04	0.01
leading baryon pol.	$\mathcal{P}_\Lambda$	—	~0.1
jet-handedness	h_j	—	$\lesssim$0.002
non-leading baryon $\mathcal{P}_t$	$\mathcal{P}_t^\Lambda$	—	~0.01
leading particle effects	r_p	—	0.15

* The world averages quoted here are dominated largely by recent LEP results which are based on a sample of 3.5 million events. It is expected that this sample will at least double in the next few years. The precisions quoted here will improve by the square root of this factor unless limited by systematic uncertainties.

6. Acknowledgments

Successful development of the SLC is the result of an immense effort by many members of the SLAC Accelerator Department and the technical staffs for more than a decade. The SLD Collaboration is grateful for these outstanding efforts on our behalf, and would like to thank them and the technical staffs of our collaborating institutions.

References

1. P. Krejcik et al., "High Intensity Bunch Length Instabilities in the SLC Damping Rings," *Proceedings of the 1993 Particle Accelerator Conference*, Washington, DC, 1993.
2. C. Adolphsen, F.-J. Decker and J. Seeman, "Flat Beams in the SLC," *Proceedings of the 1993 Particle Accelerator Conference*, Washington, DC, 1993.
3. J.T. Seeman et al., "Induced Beam Oscillations from Quadrupole Vibrations of about 2 Microns at the SLC," *Proceedings of the 1993 Particle Accelerator Conference*, Washington, DC, 1993.
4. T. Himel et al., "Adaptive Cascaded Beam-Based Feedback at the SLC," Proceedings of the 1993 Particle Accelerator Conference, Washington, DC, 1993.
5. J.T. Seeman et al., "Introduction of Trajectory Oscillations to Reduce Emittance Growth in the SLC Linac," Proceedings of the XVth International Conference on High-Energy Accelerators, Hamburg, 1992 and SLAC–PUB–5705.
6. P. Bambade et al., "Observation of Beam-Beam Deflections at the Interaction Point of the SLAC Linear Collider," Phys. Rev. Lett. **62** (1989) 2949.
7. J.E. Clendenin et al., "Performance of the SLC Polarized Electron Source with High Polarization," Proceedings of the 1993 Particle Accelerator Conference, Washington, DC, 1993.
8. T. Limberg et al., "The North Arc of the SLC as a Spin Rotator," Proceedings of the 1993 Particle Accelerator Conference, Washington, DC, 1993.
9. M. Fero et al., "The Compton Polarimeter for SLC," Proceedings of the 10th International Symposium on High-Energy Spin Physics, Nagoya, Japan, 1992 and SLAC–PUB–6026.
10. C. Prescott, "Polarization Developments," these proceedings.
11. N. Walker et al., "Third-Order Corrections to the SLC Final Focus," Proceedings of the 1993 Particle Accelerator Conference, Washington, DC, 1993.
12. P. Chen, "Disruption Effects from the Collision of Quasi-Flat Beam', Proceedings of the 1993 Particle Accelerator Conference, Washington, DC, 1993.
13. The SLD Collaboration, "First Measurement of the Left-Right Cross Section Asymmetry in Z Boson Production by e^+e^- Collisions," Phys. Rev. Lett. **70** (1993) 2515.
14. G.D. Agnew et al., "Design and Performance of the SLD Vertex Detector, a 120 MPixel Tracking System," Proceedings of the XXVI International Conference on High-Energy Physics, Dallas (1992) 1862.